CLASSIFICATION OF IGNEOUS ROCKS USING A LITHOGEOCHEMICAL ADAPTATION OF THE STRECKEISEN METHOD

Cliff Stanley

Dept. of Earth & Environmental Science, Acadia University, Wolfville, Nova Scotia, B4P 2R6, Canada, cliff.stanley@acadiau.ca

Introduction

Effective mineral exploration requires the collection of reliable geological information from outcrop and drill core. Central to this objective is accurate rock classification and the clues it provides a geochemist regarding the genesis of the target mineralization and the environment it formed in.

Unfortunately, accurate rock classification represents a significant challenge to geochemists because the diagnostic properties of rocks may not be easy to determine. Specifically, the mineral modes used in rock classification and made by visual inspection are commonly difficult to estimate, and thus susceptible to large errors. Fine-grained texture is also a significant impediment to accurate modal mineral estimates, and obscuring geological processes, such as hydrothermal alteration, metamorphism, and weathering, can change the mineralogy of rocks. All of these factors complicate rock classification and reduce its accuracy to inadequate levels.

Use of a novel igneous rock classification procedure that relies on lithogeochemical data instead of mineral modes can improve igneous rock classification accuracy. Such a technique would significantly improve the effectiveness of mineral exploration.

Methodology

Conventional Igneous Rock Classification

A very large number of igneous rock classification procedures have been proposed to facilitate both mapping of plutonic and volcanic rocks, and to investigate their environments and genesis (Meschede 1986; Sun & McDonough 1989; Pearce 1996; Hollings & Wyman 2005; Wyman & Hollings 2006). Some methods employ both major oxide and trace element geochemical concentrations to assist in: (i) assigning names to igneous rocks (i.e., classification; e.g., Le Bas et al. 1986; Winchester & Floyd 1977; Ewart 1982; Hallberg 1984; Pearce 1996), (ii) establishing their geochemical affinities (e.g., Irvine & Baragar 1971; Miyashiro 1974; Floyd & Winchester 1975; Pearce 1996; Frost & Frost 2008), and (iii) determining the tectonic environment in which they formed (e.g., Pearce & Cann 1973; Wood 1980; Pearce et al. 1981, 1984; Shervais 1982; Pearce 1983, 1996). These methods have

generally been used effectively to classify igneous rocks and provide insights into their genesis.

However, probably the most fundamental igneous rock classification method presently available is that of Streckeisen (1974; Streckeisen et al. 2002). This procedure traditionally requires quantitative volume mineral mode estimates to assign proper names to (classify) both felsic and mafic magmatic and volcanic rocks on a variety of ternary diagrams. As a result, classification using Streckeisen's technique is different from the above approaches in that it does not take advantage of the generally superior accuracy and precision that lithogeochemical data can provide. As a result, errors in estimates of mineral abundances can significantly undermine the accuracy of Streckeisen classification, forcing its application to be undertaken using expensive and time-consuming point count data or image analysis results.

One method that attempts to resolve this problem is that of (Le Maitre 1976), who used CIPW norms calculated from lithogeochemical data to classify both plutonic and volcanic rocks on Streckeisen ternary diagrams. This procedure requires conversion of the normative mass mineral proportions into the volume proportion format necessary for Streckeisen classification. Although this effort represents a laudable and rigorous attempt at igneous rock classification using lithogeochemical data, and exploits the accuracy and precision advantages that lithogeochemistry data provide, it suffers from several problems that have limited its application. First, some of the minerals used in the norm calculation (e.g., corundum, hypersthene) may not be present in the igneous rocks to be classified. Conversely, some relatively abundant igneous minerals commonly found in magmatic and volcanic rocks (e.g., biotite, hornblende, muscovite) are not normative minerals. Furthermore, none of the normative mafic minerals (olivine, hypersthene, diopside) contain Al, in contrast to the mafic minerals common to most granitoid rocks (biotite, hornblende). Unfortunately, these mineral assemblage and mineral composition differences undermine the appropriateness and relevance of this normative approach because they distort the lithogeochemical results, causing inaccuracies (biases) in subsequent classifications. As a result, Le Maitre's normative-Streckeisen ternary diagram classification method (1976) has not gained favour as a reliable classification procedure.

A New Igneous Rock Lithogeochemical Classification Method

To address the accuracy problem of mineral mode-based classification, a general lithogeochemical classification method has been developed to provide the volume-based mineral mode estimates of rocks necessary to employ Streckeisen's classification philosophy on ternary diagrams (Figure 1). This method, inspired by and representing a modification of Le Maitre's CIPW norm-based approach (1976), undertakes a novel strategy, using the set of minerals that are present in substantial proportions in the rocks to be classified to make the classification, instead of the

fixed, artificial set of normative minerals. This allows conversion of the mass-based major oxide concentrations into the volume-based mineral modes necessary for the Streckeisen classification approach (1974; Streckeisen et al. 2002). However, this procedure uses an intermediate step that first involves the transformation of major oxide concentrations into molar element numbers through the division of their corresponding molecular weights.

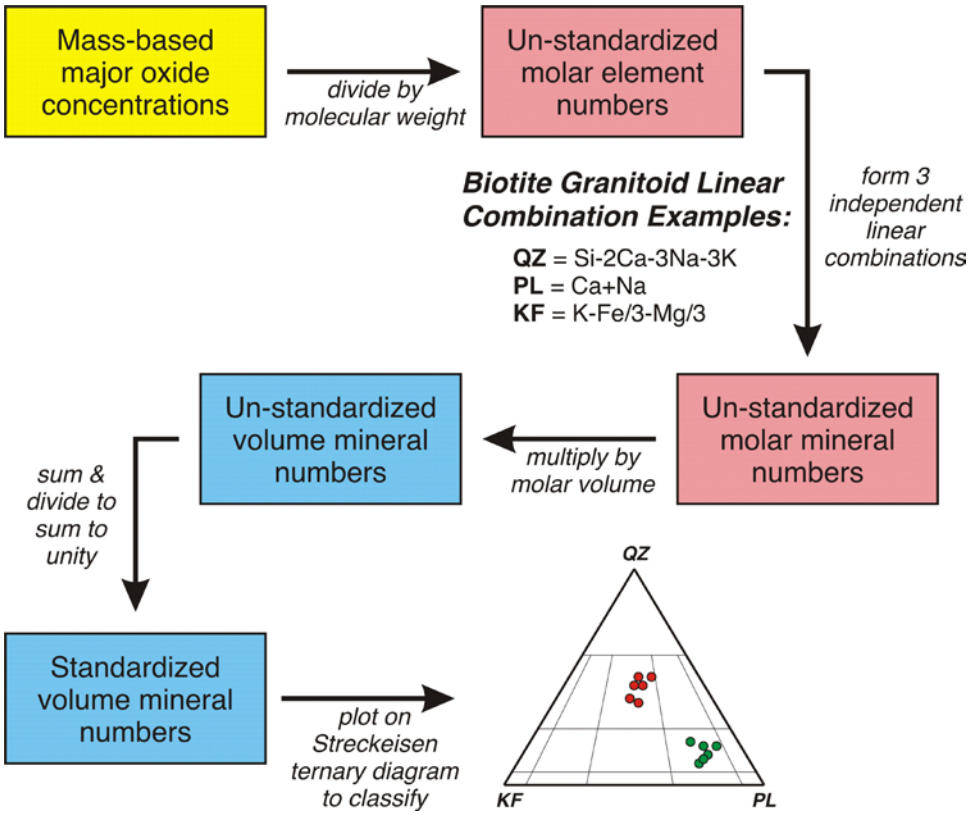

Figure 1. Flow chart illustrating the calculations used in a Streckeisen-style lithogeochemical classification. Note that the linear combinations of elements used in this example to exclusively describe quartz (*QZ*: Si-2Ca-3Na-3K), plagioclase, (*PL*: Ca+Na) and K-feldspar (*KF*: K-Fe/3-Mg/3) can be reasoned out intuitively with knowledge of the compositions of the 'essential minerals' within the rocks (in this case, quartz, plagioclase, alkali feldspar, and biotite).

These molar element numbers have the advantage of sharing the same format as mineral compositions, because both are expressed in molar terms. As a result, linear combinations of molar ***element*** numbers can be used to produce molar ***mineral*** numbers. The appropriate linear combinations to achieve this conversion are determined using matrix algebra procedures and the principles of projective geometry, and are further constrained by the compositions of the 'essential minerals' in the rocks (those minerals comprising at least 5 % of the rock – by volume – in at least 5 % of the rocks). These linear combinations are further constrained to be independent of (projections from) each other, and all of the other 'essential minerals' in the rocks. Use of these essential minerals to undertake the classification effectively amounts to the calculation of a 'custom' norm to lithogeochemically

classify the rocks using the exact mineralogy present, and thus provides a significant advantage over Le Maitre's approach (1976).

By calculating the molar mineral numbers for minerals on the vertices of ternary diagrams used in Streckeisen classification procedures (e.g., quartz, plagioclase, & alkali feldspar (QAP), and feldspathoid, plagioclase, & alkali feldspar (FAP) for granitoid intrusions; olivine, pyroxene, & plagioclase (OPP), orthopyroxene, clinopyroxene, & plagioclase (OCP), olivine, clinopyroxene, & orthopyroxene (OCO), olivine, pyroxene, hornblende (OPH), pyroxene, plagioclase, & hornblende (PPH) for mafic intrusions; 1974; Streckeisen et al. 2002), measures of the molar mineral modes of rocks can be obtained. These can then be converted into volume mineral numbers through multiplication by the corresponding molar volumes for the essential minerals, and finally standardized to sum to unity, so that they plotted on one of the Streckeisen ternary diagrams for classification.

Using matrix algebra procedures, appropriate linear combinations have been identified to allow classification on a variety of ternary diagrams employed by Streckeisen's method (1974) to classify felsic, intermediate, mafic, and ultramafic igneous rocks.

Matrix Algebra

Critical to the above lithogeochemical classification approach is the derivation of the appropriate linear combinations that convert molar element numbers into molar mineral numbers. This derivation can be achieved using MATLAB® matrix algebra software by first defining a matrix (***C***) that contains the elements describing the compositions of all essential minerals in the rocks to be classified. For example, if classification of a biotite-bearing granitoid intrusion is the objective, the rock will be classified using the QAP Streckeisen ternary diagram, and thus consider the abundances of: quartz, plagioclase, and alkali feldspar (the minerals comprising the vertices of this ternary diagram), and biotite (because it is also an essential mineral, and thus must be projected from to correctly classify the granitoid rock). As a result, the matrix ***C*** should contain the end-member compositions of these four essential minerals (quartz – QZ, anorthite – AN, albite – AB, K-feldspar – KF, phlogopite – PH, and annite – AT):

$$C = \begin{array}{c} \\ QZ \\ AN \\ AB \\ KF \\ PH \\ AT \end{array} \begin{array}{c} \begin{array}{ccccccc} Si & Al & Fe & Mg & Ca & Na & K \end{array} \\ \begin{pmatrix} 1 & 0 & 0 & 0 & 0 & 0 & 0 \\ 2 & 2 & 0 & 0 & 1 & 0 & 0 \\ 3 & 1 & 0 & 0 & 0 & 1 & 0 \\ 3 & 1 & 0 & 0 & 0 & 0 & 1 \\ 3 & 1 & 0 & 3 & 0 & 0 & 1 \\ 3 & 1 & 3 & 0 & 0 & 0 & 1 \end{pmatrix} \end{array}. \quad (1)$$

In this lithogeochemical adaptation of Streckeisen's classification approach, the molar amounts of each element in the rocks under consideration will be multiplied by three sets of unknown coefficients ($\boldsymbol{V_{QZ}}$, $\boldsymbol{V_{PL}}$, $\boldsymbol{V_{KF}}$; vectors defining linear combinations of elements) to produce quantitative estimates of the molar amounts of each mineral on the vertices of the Streckeisen ternary diagram. To make the desired linear combinations specific to these three vertex minerals, the products of the mineral composition (row) vectors in matrix $\boldsymbol{C}$ times the unknown coefficient vectors for each ternary diagram vertex ($\boldsymbol{V_{QZ}}$, $\boldsymbol{V_{PL}}$, $\boldsymbol{V_{KF}}$) must be '1' for the corresponding mineral, and '0' for all of the other essential minerals. These '0' and '1' product values are stored in matrix $\boldsymbol{P}$:

$$P = \begin{array}{c} \\ QZ \\ AN \\ AB \\ KF \\ PH \\ AN \end{array} \begin{array}{c} \begin{array}{cccc} V_{QZ} & V_{PL} & V_{KF} & V_{BT} \end{array} \\ \begin{pmatrix} 1 & 0 & 0 & 0 \\ 0 & 1 & 0 & 0 \\ 0 & 1 & 0 & 0 \\ 0 & 0 & 1 & 0 \\ 0 & 0 & 0 & 1 \\ 0 & 0 & 0 & 1 \end{pmatrix} \end{array}, \tag{2}$$

Furthermore, in order to ensure that the presence of biotite does not influence the classification, the corresponding dot products for biotite (its end-members phlogopite and annite) should all be '0' in the three column vectors defining the ternary diagram ($\boldsymbol{V_{QZ}}$, $\boldsymbol{V_{PL}}$, $\boldsymbol{V_{KF}}$). Lastly, an extra vector ($\boldsymbol{V_{BT}}$) can be used to describe the amount of biotite using a linear combination vector containing values of '1' for phlogopite and annite, and '0' elsewhere so that a full estimate of the mineral mode of the rock can be obtained.

Appending the $\boldsymbol{C}$ and $\boldsymbol{P}$ matrices side-by-side, we obtain:

$$(C \mid P) = \begin{array}{c} \\ QZ \\ AN \\ AB \\ KF \\ PH \\ AT \end{array} \begin{array}{c} \begin{array}{ccccccc|cccc} Si & Al & Fe & Mg & Ca & Na & K & V_{QZ} & V_{PL} & V_{KF} & V_{BT} \end{array} \\ \left(\begin{array}{ccccccc|cccc} 1 & 0 & 0 & 0 & 0 & 0 & 0 & 1 & 0 & 0 & 0 \\ 2 & 2 & 0 & 0 & 1 & 0 & 0 & 0 & 1 & 0 & 0 \\ 3 & 1 & 0 & 0 & 0 & 1 & 0 & 0 & 1 & 0 & 0 \\ 3 & 1 & 0 & 0 & 0 & 0 & 1 & 0 & 0 & 1 & 0 \\ 3 & 1 & 0 & 3 & 0 & 0 & 1 & 0 & 0 & 0 & 1 \\ 3 & 1 & 3 & 0 & 0 & 0 & 1 & 0 & 0 & 0 & 1 \end{array}\right) \end{array}. \tag{3}$$

Then, deriving the reduced row echelon form of this composite matrix results in:

$$RREF(C \mid P) = (I \mid N \mid A) = \left(\begin{array}{cccccc|c|cccc} 1 & 0 & 0 & 0 & 0 & 0 & 0 & 1 & 0 & 0 & 0 \\ 0 & 1 & 0 & 0 & 0 & 0 & 1 & -3 & 0 & 1 & 0 \\ 0 & 0 & 1 & 0 & 0 & 0 & 0 & 0 & 0 & -1/3 & 1/3 \\ 0 & 0 & 0 & 1 & 0 & 0 & 0 & 0 & 0 & -1/3 & 1/3 \\ 0 & 0 & 0 & 0 & 1 & 0 & -2 & 4 & 1 & -2 & 0 \\ 0 & 0 & 0 & 0 & 0 & 1 & -1 & 0 & 1 & -1 & 0 \end{array}\right). \tag{4}$$

Finally, dropping the leading identity matrix (***I***), and appending a negative identity matrix of size (1 × 1) to the bottom of the null space matrix (***N***) and a zero matrix of size (1 × 4) to the bottom of the ***A*** matrix results in:

$$\begin{pmatrix} N & A \\ -I & 0 \end{pmatrix} = \begin{array}{c} \\ Si \\ Al \\ Fe \\ Mg \\ Ca \\ Na \\ K \end{array} \begin{array}{c} \begin{array}{ccccc} V_N & V_{QZ} & V_{PL} & V_{KF} & V_{BT} \end{array} \\ \left(\begin{array}{c|cccc} 0 & 1 & 0 & 0 & 0 \\ 1 & -3 & 0 & 1 & 0 \\ 0 & 0 & 0 & -1/3 & 1/3 \\ 0 & 0 & 0 & -1/3 & 1/3 \\ -2 & 4 & 1 & -2 & 0 \\ \hdashline -1 & 0 & 1 & -1 & 0 \\ \hdashline -1 & 0 & 0 & 0 & 0 \end{array}\right) \end{array} . \tag{5}$$

The resulting matrix contains two types of column vectors. Vector $\boldsymbol{V_N}$ is a basis for the null space of matrix ***C***, and so is perpendicular to all of its row vectors. Consequently, the dot products of the row vectors in ***C*** and $\boldsymbol{V_N}$ all equal zero, and $\boldsymbol{V_N}$ is a non-trivial (non-zero) solution (***A***) to the homogeneous equation $\boldsymbol{C \times A = 0}$:

$$C \times A = \begin{array}{c} \\ QZ \\ AN \\ AB \\ KF \\ PH \\ AT \end{array} \begin{array}{c} \begin{array}{ccccccc} Si & Al & Fe & Mg & Ca & Na & K \end{array} \\ \begin{pmatrix} 1 & 0 & 0 & 0 & 0 & 0 & 0 \\ 2 & 2 & 0 & 0 & 1 & 0 & 0 \\ 3 & 1 & 0 & 0 & 0 & 1 & 0 \\ 3 & 1 & 0 & 0 & 0 & 0 & 1 \\ 3 & 1 & 0 & 3 & 0 & 0 & 1 \\ 3 & 1 & 3 & 0 & 0 & 0 & 1 \end{pmatrix} \end{array} \times \begin{array}{c} \begin{array}{c} V_N \end{array} \\ \begin{pmatrix} 0 \\ 1 \\ 0 \\ 0 \\ -2 \\ -1 \\ -1 \end{pmatrix} \end{array} \begin{array}{c} \\ Si \\ Al \\ Fe \\ Mg \\ Ca \\ Na \\ K \end{array} = \begin{array}{c} \\ QZ \\ AN \\ AB \\ KF \\ PH \\ AT \end{array} \begin{array}{c} \begin{array}{c} \end{array} \\ \begin{pmatrix} 0 \\ 0 \\ 0 \\ 0 \\ 0 \\ 0 \end{pmatrix} \end{array} = 0 . \tag{6}$$

The other four column vectors ($\boldsymbol{V_{QZ}}$, $\boldsymbol{V_{PL}}$, $\boldsymbol{V_{KF}}$, and $\boldsymbol{V_{BT}}$) describe linear combinations of elements that can be used to convert the molar element numbers into corresponding molar mineral numbers for quartz, plagioclase, alkali feldspar, and biotite. Each of these vectors, when multiplied by the corresponding row vector(s) in matrix ***C***, will equal one, but will equal zero when multiplied by any of the other row vectors (as defined originally in matrix ***P***). As a result, these other column vectors ($\boldsymbol{V_{QZ}}$, $\boldsymbol{V_{PL}}$, $\boldsymbol{V_{KF}}$, and $\boldsymbol{V_{BT}}$) collectively are the solution (***A***) to the characteristic matrix equation $\boldsymbol{C \times A = P}$. Thus:

$$C \times A = \begin{array}{c} \\ QZ \\ AN \\ AB \\ KF \\ PH \\ AT \end{array} \begin{array}{c} \begin{array}{ccccccc} Si & Al & Fe & Mg & Ca & Na & K \end{array} \\ \begin{pmatrix} 1 & 0 & 0 & 0 & 0 & 0 & 0 \\ 2 & 2 & 0 & 0 & 1 & 0 & 0 \\ 3 & 1 & 0 & 0 & 0 & 1 & 0 \\ 3 & 1 & 0 & 0 & 0 & 0 & 1 \\ 3 & 1 & 0 & 3 & 0 & 0 & 1 \\ 3 & 1 & 3 & 0 & 0 & 0 & 1 \end{pmatrix} \end{array} \times \begin{array}{c} \begin{array}{cccc} V_{QZ} & V_{PL} & V_{KF} & V_{BT} \end{array} \\ \begin{pmatrix} 1 & 0 & 0 & 0 \\ -3 & 0 & 1 & 0 \\ 0 & 0 & -1/3 & 1/3 \\ 0 & 0 & -1/3 & 1/3 \\ 4 & 1 & -2 & 0 \\ 0 & 1 & -1 & 0 \\ 0 & 0 & 0 & 0 \end{pmatrix} \end{array} \begin{array}{c} \\ Si \\ Al \\ Fe \\ Mg \\ Ca \\ Na \\ K \end{array} = \begin{array}{c} \\ QZ \\ AN \\ AB \\ KF \\ PH \\ AT \end{array} \begin{array}{c} \begin{array}{cccc} V_{QZ} & V_{PL} & V_{KF} & V_{BT} \end{array} \\ \begin{pmatrix} 1 & 0 & 0 & 0 \\ 0 & 1 & 0 & 0 \\ 0 & 1 & 0 & 0 \\ 0 & 0 & 1 & 0 \\ 0 & 0 & 0 & 1 \\ 0 & 0 & 0 & 1 \end{pmatrix} \end{array} = P . \tag{7}$$

Clearly, these four mineral column vectors each create projections (have dot products of 0) from all other minerals in the granite, and thus the first three, when multiplied by the corresponding molar element numbers, will produce independent molar mineral numbers that can be multiplied by their corresponding molar volumes, standardized to unity, and plotted on the QAP Streckeisen ternary diagram for classification.

A fundamental feature of this matrix algebra approach is that, in this and many other cases, there is commonly more than one set of possible linear combinations (***V*****$_{QZ}$**, ***V*****$_{PL}$**, ***V*****$_{KF}$**, ***V*****$_{BT}$**) that solve the characteristic equation. In this biotite granitoid example, because the null space matrix (***V*****$_N$**) exists, there are an infinite number of linear combinations for quartz, plagioclase, alkali feldspar, and biotite. These infinite solutions consist of the set of all possible linear combinations of each mineral column vector (***V*****$_{QZ}$**, ***V*****$_{PL}$**, ***V*****$_{KF}$**, ***V*****$_{BT}$**) and the null space vector (***V*****$_N$**; e.g., ***aV*****$_N$ + *bV*$_{QZ}$**, where a and b are coefficients). For example, if ***a = 3*** and ***b = 1***, then the resulting linear combination for an alternative linear combination for quartz (***V*****$_{QZ*}$**) is:

$$V_{QZ*} = 3V_N + 1V_{QZ} = 3\times \begin{matrix} V_N \\ \begin{pmatrix} 0 \\ 1 \\ 0 \\ 0 \\ -2 \\ -1 \\ -1 \end{pmatrix} \end{matrix} \begin{matrix} Si \\ Al \\ Fe \\ Mg \\ Ca \\ Na \\ K \end{matrix} + 1\times \begin{matrix} V_{QZ} \\ \begin{pmatrix} 1 \\ -3 \\ 0 \\ 0 \\ 4 \\ 0 \\ 0 \end{pmatrix} \end{matrix} = \begin{matrix} 3V_N \\ \begin{pmatrix} 0 \\ 3 \\ 0 \\ 0 \\ -6 \\ -3 \\ -3 \end{pmatrix} \end{matrix} + \begin{matrix} V_{QZ} \\ \begin{pmatrix} 1 \\ -3 \\ 0 \\ 0 \\ 4 \\ 0 \\ 0 \end{pmatrix} \end{matrix} = \begin{matrix} Si \\ Al \\ Fe \\ Mg \\ Ca \\ Na \\ K \end{matrix} \begin{matrix} V_{QZ*} \\ \begin{pmatrix} 1 \\ 0 \\ 0 \\ 0 \\ -2 \\ -3 \\ -3 \end{pmatrix} \end{matrix} . \tag{8}$$

This linear combination (***V*****$_{QZ*}$**) produces exactly the results as the original linear combination for quartz (***V*****$_{QZ}$**) when multiplied by the quartz, plagioclase, alkali feldspar, and biotite compositions (row vectors in matrix ***C***), and is exactly the intuitive linear combination presented in Figure 1 (Si-2Ca-3Na-3K; note that the linear combination – ***V*****$_{PL}$** – for plagioclase in this example is the same linear combination for plagioclase presented in Figure 1; Ca+Na). Similarly, if we use a linear combination of the null space (***V*****$_N$**) and alkali feldspar vectors (***V*****$_{KF}$**; ***cV*****$_N$ + *dV*$_{KF}$**), where ***c = -1*** and ***d = 1***, we obtain an alternative ***V*****$_{KF*}$** vector:

$$V_{KF*} = -1V_N + 1V_{AF} = -1\times \begin{matrix} V_N \\ \begin{pmatrix} 0 \\ 1 \\ 0 \\ 0 \\ -2 \\ -1 \\ -1 \end{pmatrix} \end{matrix} \begin{matrix} Si \\ Al \\ Fe \\ Mg \\ Ca \\ Na \\ K \end{matrix} + 1\times \begin{matrix} V_{KF} \\ \begin{pmatrix} 0 \\ 1 \\ -1/3 \\ -1/3 \\ -2 \\ -1 \\ 0 \end{pmatrix} \end{matrix} = \begin{matrix} -1V_N \\ \begin{pmatrix} 0 \\ -1 \\ 0 \\ 0 \\ 2 \\ 1 \\ 1 \end{pmatrix} \end{matrix} + \begin{matrix} V_{KF} \\ \begin{pmatrix} 0 \\ 1 \\ -1/3 \\ -1/3 \\ -2 \\ -1 \\ 0 \end{pmatrix} \end{matrix} = \begin{matrix} Si \\ Al \\ Fe \\ Mg \\ Ca \\ Na \\ K \end{matrix} \begin{matrix} V_{KF*} \\ \begin{pmatrix} 0 \\ 0 \\ -1/3 \\ -1/3 \\ 0 \\ 0 \\ 1 \end{pmatrix} \end{matrix} . \tag{9}$$

Again, this linear combination (***V*****$_{KF*}$**) is the same as the intuitive linear combination for alkali feldspar presented in Figure 1 (K-Fe/3-Mg/3).

Finally, because there are an infinite number of linear combinations that can be used to convert molar element numbers into molar mineral numbers, it is useful to create a labelling system for these matrix equation solutions. In the above derivation, the original linear combinations are (from Equation 7):

$$A_{K-absent} = \begin{array}{c} \\ Si \\ Al \\ Fe \\ Mg \\ Ca \\ Na \\ K \end{array} \begin{array}{c} \begin{array}{cccc} V_{QZ} & V_{PL} & V_{KF} & V_{BT} \end{array} \\ \begin{pmatrix} 1 & 0 & 0 & 0 \\ -3 & 0 & 1 & 0 \\ 0 & 0 & -1/3 & 1/3 \\ 0 & 0 & -1/3 & 1/3 \\ 4 & 1 & -2 & 0 \\ 0 & 1 & -1 & 0 \\ 0 & 0 & 0 & 0 \end{pmatrix} \end{array}. \tag{10}$$

In this case, the one characteristic common to all four mineral column vectors is that the coefficients for K are all zero. As a result, we refer to this set of linear combinations as the 'K-absent' solution, borrowing this nomenclature from metamorphic petrology. The alternative solution (***A****) presented in Figure 1, utilizing $\boldsymbol{V_{QZ*}}$ and $\boldsymbol{V_{KF*}}$ instead of $\boldsymbol{V_{QZ}}$ and $\boldsymbol{V_{KF}}$, is:

$$A^*_{Al-absent} = \begin{array}{c} \\ Si \\ Al \\ Fe \\ Mg \\ Ca \\ Na \\ K \end{array} \begin{array}{c} \begin{array}{cccc} V_{QZ*} & V_{PL} & V_{KF*} & V_{BT} \end{array} \\ \begin{pmatrix} 1 & 0 & 0 & 0 \\ 0 & 0 & 0 & 0 \\ 0 & 0 & -1/3 & 1/3 \\ 0 & 0 & -1/3 & 1/3 \\ -2 & 1 & 0 & 0 \\ -3 & 1 & 0 & 0 \\ -3 & 0 & 1 & 0 \end{pmatrix} \end{array}. \tag{11}$$

This solution has zero coefficients for Al in all four mineral vectors, and thus is named the 'Al-absent' solution. Analogous linear combinations can be derived and named as 'Ca-absent' (where $\boldsymbol{V_{QZ**} = V_{QZ} + 2\,V_N}$ and $\boldsymbol{V_{PL*} = V_{PL} + ½\,V_N}$) 'Na-absent' (where $\boldsymbol{V_{PL**} = V_{PL} + V_N}$) solutions:

$$A^*_{Ca-absent} = \begin{array}{c} \\ Si \\ Al \\ Fe \\ Mg \\ Ca \\ Na \\ K \end{array} \begin{array}{c} \begin{array}{cccc} V_{QZ**} & V_{PL*} & V_{KF*} & V_{BT} \end{array} \\ \begin{pmatrix} 1 & 0 & 0 & 0 \\ -1 & 1/2 & 0 & 0 \\ 0 & 0 & -1/3 & 1/3 \\ 0 & 0 & -1/3 & 1/3 \\ 0 & 0 & 0 & 0 \\ -2 & 1/2 & 0 & 0 \\ -2 & -1/2 & 1 & 0 \end{pmatrix} \end{array}, \tag{12}$$

and:

$$A^*_{Na-absent} = \begin{array}{c} \\ Si \\ Al \\ Fe \\ Mg \\ Ca \\ Na \\ K \end{array} \begin{array}{c} \begin{array}{cccc} V_{QZ} & V_{PL**} & V_{KF} & V_{BT} \end{array} \\ \begin{pmatrix} 1 & 0 & 0 & 0 \\ -3 & 1 & 0 & 0 \\ 0 & 0 & -1/3 & 1/3 \\ 0 & 0 & -1/3 & 1/3 \\ 4 & -1 & 0 & 0 \\ 0 & 0 & 0 & 0 \\ 0 & -1 & 1 & 0 \end{pmatrix} \end{array} . \quad (13)$$

Note that a 'Si-absent' solution cannot be derived because there is only one element analyzed in quartz (Si) so it must be used to describe quartz and thus can't be 'absent'. Similarly, a 'Fe-Mg-absent' solution cannot be derived because no linear combination of $\boldsymbol{V_N}$ and the four original mineral vectors can produce a result that is has zero coefficients for Fe and Mg.

Clearly, an advantage of having multiple ways of calculating the abundances of the ternary diagram vertex minerals is that if one or more elements haven't been analyzed, or cross-cutting veins or hydrothermal alteration affect an element abundance, classification can still be undertaken using solutions that do not involve the problematic element. Another advantage of this approach is that, although ideal compositions of the essential minerals have been used in this example, the actual compositions, determined by electron microprobe analysis, could be used to derive the appropriate linear combinations. Although this would likely result in non-integer coefficients in the linear combinations, it would precisely tailor the classification to the compositions of the minerals present in the rocks.

Discussion

To illustrate how lithogeochemical classification can be undertaken using this Streckeisen-style approach, three examples are presented below involving classification of metaluminous and alkalic granitoids and a layered mafic-ultramafic intrusion.

Metaluminous Sloggetts Pluton Granitoid Rock, New South Wales, Australia

The first classification example involves a single rock composition (OZCHEM # 72464; Champion et al. 2007) from the Sloggetts pluton, a 7 km^2 intrusion within the Oberon batholith in the Lachlan fold belt of New South Wales, Australia (Glen et al. 2006; Pogson & Watkins 1998; McCormack 1985). This rock contains coarsely porphyritic pink alkali feldspar (OR_{81} to OR_{88}) in a coarse grained groundmass of quartz, plagioclase (AN_{26} to AN_{29}), alkali feldspar (OR_{73}), and biotite. In addition, it was analyzed for major oxides by fusion-XRF methods, and has a molar $Al_2O_3/(CaO+Na_2O+K_2O)$ ratio = 1.02. Consequently, it is described as having metaluminous affinities (McCormack 1985).

The abundances of quartz, plagioclase, alkali feldspar, and biotite in this Sloggett pluton sample are all greater than 5 %, and so likely control the composition of the intrusion. Although minor to trace amounts of igneous magnetite, zircon, apatite and titanite are also present, these occur in concentrations far less than 5 volume % (Glen et al. 2006; Pogson & Watkins 1998; McCormack 1985). Deuteric alteration has caused the incipient replacement of plagioclase cores and rims by sericite, and biotite by chlorite and epidote, and minor, thin calcite veins locally cut the granitoid (McCormack 1985); however, none of these alteration minerals exist in concentrations exceeding 5 %, and thus are not likely to substantially influence the rock composition or resulting classification.

Obviously, lithogeochemical classification of this Sloggett pluton sample can be undertaken using any set of solution vectors presented in or derivable from the above matrix algebra example. As a result, classification has been undertaken in four ways, and the results acquired using the Al-, Ca-, Na-, and K-absent linear combinations in Equations 10 through 13 are presented in Figure 2.

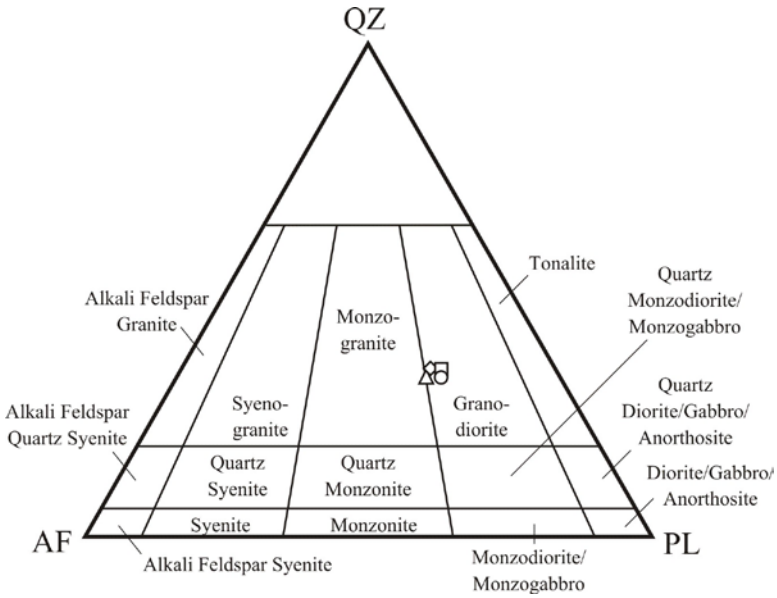

Figure 2. Example of a Steckeisen-style lithogeochemical classification for a sample of the Sloggetts pluton of the Oberon batholith in the Lachlan fold belt of New South Wales, Australia (Glen et al. 2006; Pogson & Watkins 1998; McCormack 1985). The four symbols correspond to the Al-absent (diamond), Ca-absent (square), Na-absent (circle), and K-absent (triangle) classifications, and all provide exactly the same result : *granodiorite*.

Figure 2 illustrates that the Sloggett pluton sample is clearly classified as 'granodiorite' by the Streckeisen-type lithogeochemical classification method, as all possible solutions result in the exact same result. Interestingly, this sample was originally classified as 'biotite granite' by Stuart-Smith (Glen et al. 2006) based on hand sample descriptions, and 'adamellite' by McCormack (1985) based on thin

section point counts, neither of which are substantially different from this lithogeochemical classification.

Alkaline Emerald Lake Pluton Granitoid Rock, Yukon, Canada

The Mid-Cretaceous composite Emerald Lake pluton occurs in southeastern Yukon, Canada, and is part of the alkalic Tombstone plutonic suite. Mapping of this elongate body indicates that it consists of four phases: augite syenite (AS), hornblende quartz syenite (HQS), hornblende quartz monzonite (HQM), and biotite granite (BG), with gradational contacts only between the HQS and HQM phases and cross-cutting contacts between the others (Smit 1984; Smit et al. 1985; Duncan et al. 1998a, 1998b; Duncan 1999; Coulson et al. 2001, 2002; Figure 3).

Thirty-six 1 kg samples from these four phases were analyzed by fusion-XRF methods for major oxides, and were petrographically examined in thin section, and point counted to determine their mineral modes and classifications (Duncan 1999). Point count results are presented in Figure 4.

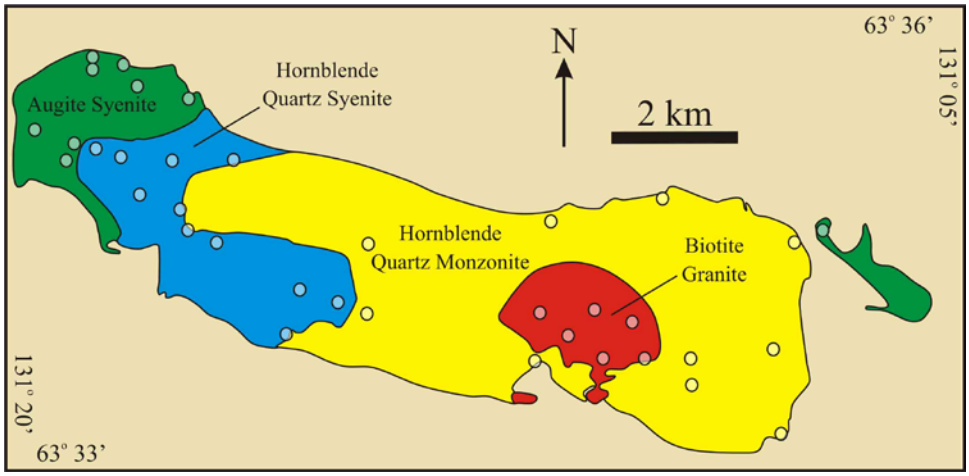

Figure 3. Geology of the Emerald Lake pluton, Yukon, after Duncan (1999) and Coulson et al. (2001, 2002), with lithogeochemical sample locations (circles).

Classification of these samples was also undertaken using the lithogeochemical strategy described above, except that the essential mineral suites used for each unit were different, as defined by their 'essential mineral assemblages': quartz, alkali feldspar, plagioclase, clinopyroxene (CP) and Na-rich hornblende (defined by the pargasite (PG) end-member) were used for AS, so the linear combinations used are:

$$A_{QZ-PL-KF-CP-PG} = \begin{array}{c} \\ Si \\ Al \\ Fe \\ Mg \\ Ca \\ Na \\ K \end{array} \begin{array}{c} \begin{array}{ccccc} V_{QZ} & V_{PL} & V_{KF} & V_{CP} & V_{PG} \end{array} \\ \begin{pmatrix} 1 & 0 & 0 & 0 & 0 \\ 1/6 & 1/6 & -1/6 & -2/3 & 1/6 \\ 1/3 & -2/3 & -1/3 & -1/3 & 1/3 \\ 1/3 & -2/3 & -1/3 & -1/3 & 1/3 \\ -7/3 & 2/3 & 1/3 & 4/3 & -1/3 \\ -19/6 & 5/6 & 7/6 & 2/3 & -1/6 \\ -19/6 & -1/6 & 7/6 & 2/3 & -1/6 \end{pmatrix} \end{array}, \quad (14)$$

quartz, alkali feldspar, plagioclase and hornblende (defined by actinolite (AC) and pargasite end-members) were used for HQS and HQM, so the linear combinations are:

$$A_{QZ-PL-KF-AC-PG} = \begin{array}{c} \\ Si \\ Al \\ Fe \\ Mg \\ Ca \\ Na \\ K \end{array} \begin{array}{c} \begin{array}{ccccc} V_{QZ} & V_{PL} & V_{KF} & V_{AC} & V_{PG} \end{array} \\ \begin{pmatrix} 1 & 0 & 0 & 0 & 0 \\ 7/2 & -7/6 & -5/6 & -2/3 & 5/6 \\ 2 & -4/3 & -2/3 & -1/3 & 2/3 \\ 2 & -4/3 & -2/3 & -1/3 & 2/3 \\ -9 & 10/3 & 5/3 & 4/3 & -7/6 \\ -13/2 & 13/6 & 11/6 & 2/3 & -5/6 \\ -13/2 & 7/6 & 11/6 & 2/3 & -5/6 \end{pmatrix} \end{array}, \quad (15)$$

and quartz, alkali feldspar, plagioclase and biotite were used for BG, so the linear combinations used were the K-absent solution (Equation 10). Results for these Streckeisen-style lithogeochemical classifications are presented in Figure 5.

A comparison of Figure 4 (petrography) and Figure 5 (lithogeochemistry) reveals several important conclusions. First, the rock compositions on Figure 5 are more clustered within lithologies (exhibiting lower modal variance), and these clusters are more separated between lithologies, than the data in Figure 4. This indicates that the lithogeochemical samples are likely substantially more representative than the thin sections used to estimate the mineral modes by point counting. In fact, based on the masses of these two samples (thin sections: ~0.065 g; lithogeochemical samples: ~1000 g), the lithogeochemical samples are more than 15,000 times larger, and thus their sampling variance is 15,000 times smaller (Stanley 2007), resulting in a far more consistent classification. Second, the HQS and HQM compositions overlap in Figure 5, and are distinct from the AS and BG compositions. These features cannot be recognized on Figure 4, as the data are overlapping and far more dispersed across the diagram. The overlapping and non-overlapping relationships between phases on Figure 5 are entirely consistent with the contact relationships between these phases in the Emerald Lake pluton, as the HQS and HQM are the only two phases with a gradational contact, suggesting a more intimate igneous relationship.

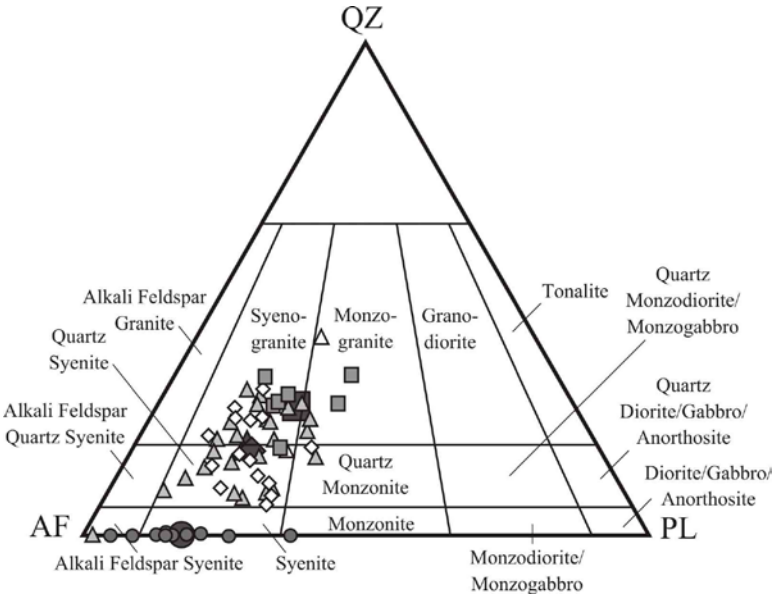

Figure 4. A silica-saturated Streckeisen ternary diagram illustrating the modal compositions of augite syenite (circles), hornblende quartz syenite (diamonds), hornblende quartz monzonite (triangles) and biotite granite (squares) as determined from point counting of thin sections. Large, dark grey symbols are the corresponding average modes for each lithology (data from Duncan 1999; Coulson et al. 2001, 2002).

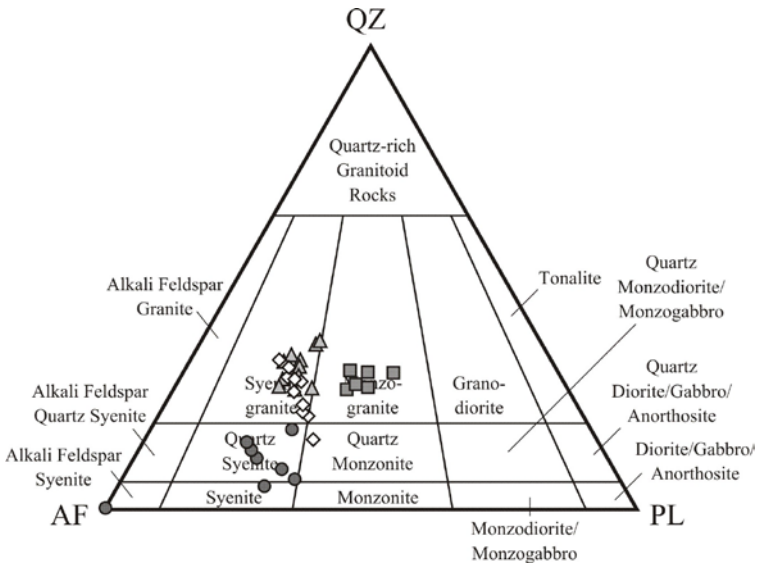

Figure 5. Silica-saturated Streckeisen ternary diagram illustrating the granitic compositions for rocks from the Emerald Lake pluton, Tombstone suite, Yukon, Canada (data from Duncan 1999; Coulson et al. 2001, 2002) calculated using the lithogeochemistry procedure described above. Symbols are the same as in Figure 4.

Lastly, samples of AS on Figure 4 plot in a location suggesting it has no quartz in its mode. This is not the case in Figure 5, as significant quartz is predicted based on the rock compositions, and this alters the classification for this lithology

from augite syenite to 'augite quartz syenite'. Similarly, the HQS and HQM units largely plot in the syenogranite field and overlap substantially, so they should probably be re-classified as a single unit as 'hornblende syenogranite'. Finally, the biotite granite samples plot in the monzogranite field, so they should likewise be re-classified as 'biotite monzogranite'. In conclusion, based on the above observations, the lithogeochemical classification employed and plotted on a Streckeisen ternary diagram appears to produce a far more representative and at least as accurate a classification as thin section point counting results for rocks from the Emerald Lake pluton.

Mafic-Ultramafic Stillwater Layered Intrusion, Montana, USA

The Stillwater complex, located in the Tobacco Root Mountains of southern Montana, is a late Archean layered mafic-ultramafic intrusion composed of three parts: (i) a Basal Series consisting of mafic dykes and noritic rocks approximately 100 m thick, (ii) an overlying 2200 m thick Ultramafic Series consisting of olivine-, and olivine+orthopyroxene-bearing cumulate rocks in its lower 1000 m, and orthopyroxene-bearing cumulate rocks, locally hosting chromitite, in the upper 1200 m, and (iii) a 4300 m thick superjacent Banded Series consisting of largely plagioclase cumulates subdivided into three parts (Lower, Middle, and Upper; McCallum et al. 1980). The Middle Banded Series is approximately 800 m thick and contains a thick anorthosite cumulate zone between two sequences of olivine-bearing cumulate rocks (OB-3 and OB-4). These rocks have been examined in detail (Meurier 1995; Meurier & Boudreau 1996, 1998), and contain anothositic, troctolitic, olivine gabbroic and gabbronoritic lithologies (Figure 6).

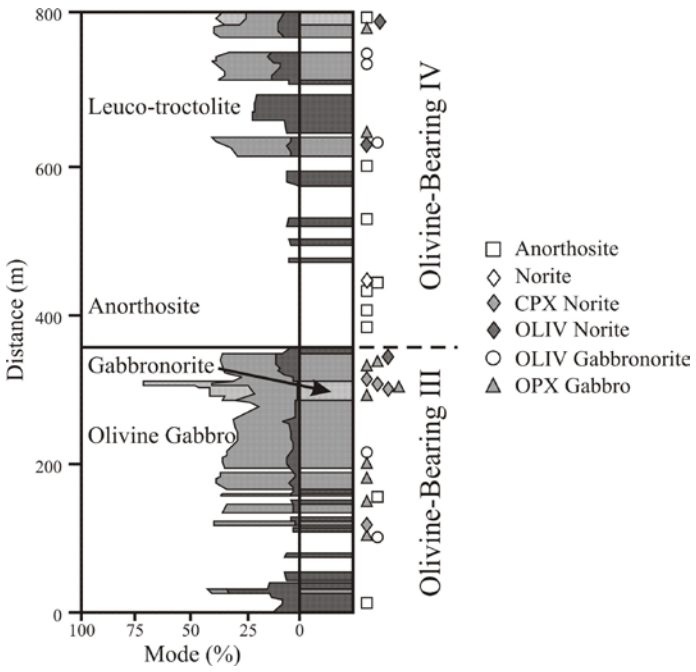

Figure 6. Stratigraphy, modal abundances, sample locations and lithologies of lithogeochemical samples from the Middle Banded Series of the Stillwater complex, Montana (after Meurier 1995).

Two surface traverses through the Middle Banded Series have provided 96 un-weathered (2 kg) rock samples from a continuous section for study (Meurier 1995). Petrographic classification (olivine, plagioclase, clinopyroxene and orthopyroxene) of these samples was undertaken using image analysis of enlarged photographs of 2 × 4 cm thin sections as input into a conventional Streckeisen classification (Streckeisen 1974; Streckeisen et al. 2002). Average grain sizes were 2 mm, so approximately 200 grains were present on each thin section. These estimates indicate that the samples consist of anorthosite, troctolite, norite, olivine norite, clinopyroxene norite, olivine gabbronorite, gabbro, olivine gabbro, and orthopyroxene gabbro. Results are presented on the two ternary diagrams (OPP and OCP) of Figure 7.

Fusion-ICP analyses of 250 g powders of these same rocks (Meurier 1995; Meurier & Boudreau 1996, 1998) were subjected to the Streckeisen-style lithogeochemical classification procedures described above, using olivine, plagioclase, orthopyroxene, and clinopyroxene as essential minerals, and thus linear combinations of:

$$A_{OL-OP-CP-PL} = \begin{array}{c} \\ Si \\ Al \\ Fe \\ Mg \\ Ca \\ Na \end{array} \begin{array}{c} \begin{array}{cccc} V_{OL} & V_{OP} & V_{CP} & V_{PL} \end{array} \\ \begin{pmatrix} -1 & 1 & 0 & 0 \\ 1/2 & -1/4 & -1/2 & 1/2 \\ 1 & -1/2 & 0 & 0 \\ 1 & -1/2 & 0 & 0 \\ 1 & -3/2 & 1 & 0 \\ 5/2 & -11/4 & 1/2 & 1/2 \end{pmatrix} \end{array} . \tag{16}$$

The resulting lithogeochemical classifications are presented in Figure 8.

Clearly, comparison of Stillwater complex petrographic classifications (Figure 7) and lithogeochemical classifications (Figure 8) revels no significant differences. Rocks classified by point counting are consistent with the lithogeochemical classifications, and quantitative results exhibit high correlations (Figure 9).

The only significant discrepancy between the modal estimates in Figure 9 is an under-estimation bias in clinopyroxene, and an over-estimation bias in plagioclase by the lithogeochemical classification method. This is probably due to the fact that the clinopyroxene composition in these rocks is sub-calcic (occurring as augite). Because the lithogeochemical classification considered only ideal diopsite-hedenbergite as clinopyroxene, the lithogeochemical classification errantly recognizes some of the augite present in these rocks as orthopyroxene instead of clinopyroxene.

Consequently, the amount of clinopyroxene in these rocks is under-estimated, causing plagioclase modes to be over-estimated due to the closure effect. This discrepancy can easily be avoided by using augite (sub-calcic clinopyroxene) compositions in the mineral composition matrix (***C***; constrained by electron

microprobe analysis), instead of the ideal composition used in this example. Nevertheless, the impact that an inaccurate clinopyroxene composition has on the classification procedure appears to be negligible, so if lithogeochemical data is available, substantial time and cost savings can be achieved using this Streckeisen-type lithogeochemical classification method instead of point counting.

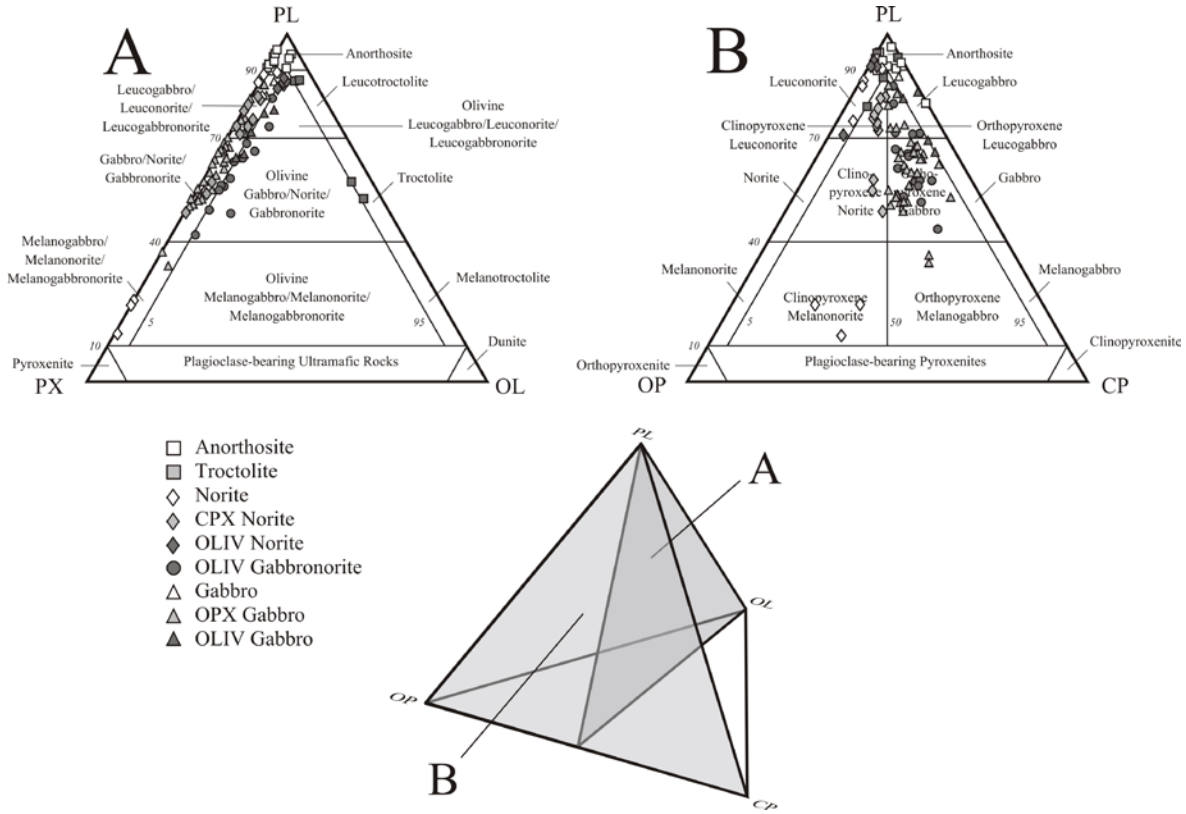

Figure 7. Image analysis results from enlarged thin section photographs from Stillwater complex rock samples plotted on two ternary Streckeisen diagrams used to classify non-amphibole-bearing mafic and ultramafic rocks (A – pyroxene, olivine, plagioclase; B – orthopyroxene, clinopyroxene, plagioclase; data from Meurier 1995).

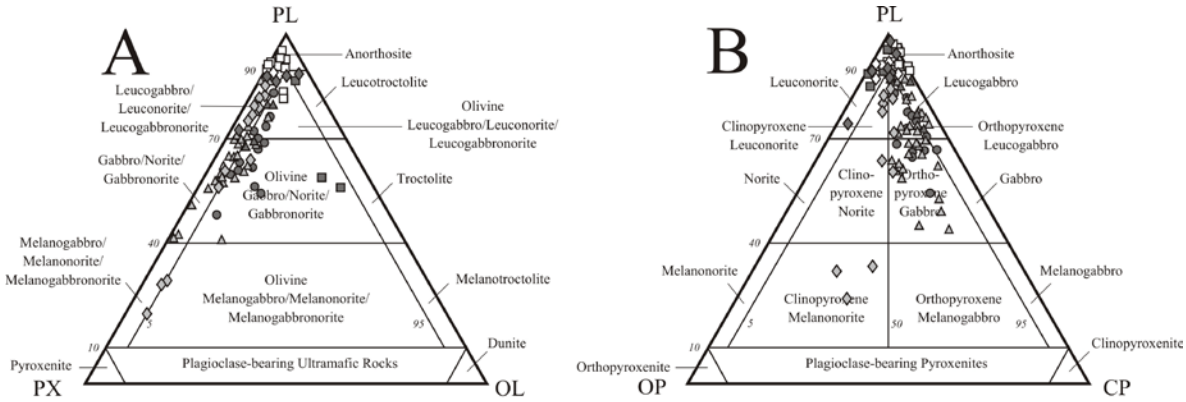

Figure 8. Streckeisen-style lithogeochemical classification results presented on the same two ternary diagrams as Figure 7. Lithology symbols are as defined in Figure 6 (data from Meurier 1995 and Meurier & Boudreau 1996, 1998).

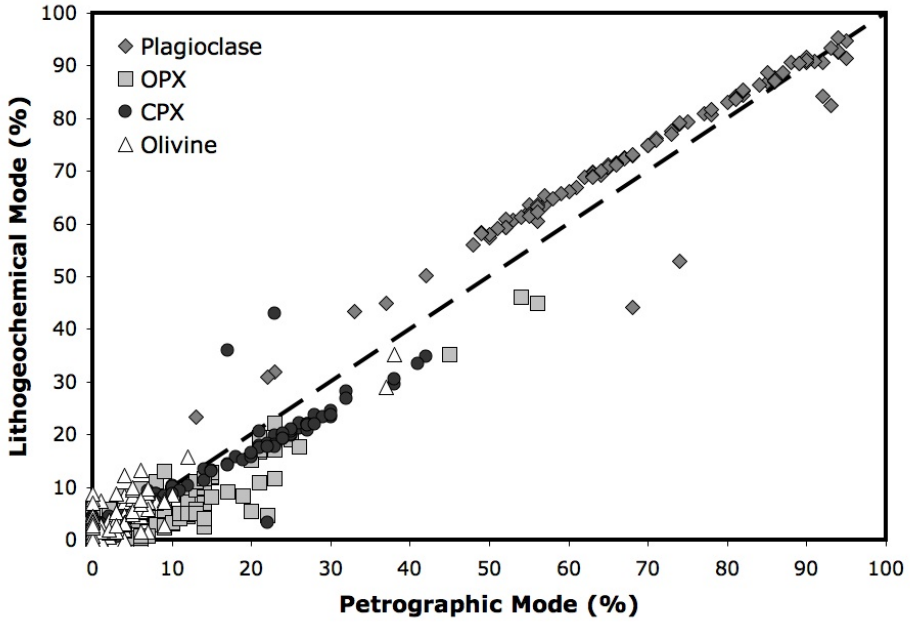

Figure 9. Scatterplot of point count and lithogeochemically-derived modes for olivine (R = 0.85), plagioclase (R = 0.96), orthopyroxene (R = 0.44), and clinopyroxene (R = 0.40; data from Meurier 1995, Meurier & Boudreau 1996, 1998).

Conclusions

The above-described Streckeisen-style igneous rock lithogeochemical classification method was originally conceived by the author in 2007, and has since undergone 7 years of testing in a variety of ways and using a large number of lithogeochemical datasets with comprehensive petrographic ground truth information in order to assess its effectiveness. Three examples of these tests are presented above. Positive (accurate, precise, consistent, robust, and conclusive) classification results have been obtained for a number of other felsic alkaline, peraluminous, and metaluminous magmatic rocks, as well as a number of other mafic alkaline, calc-alkaline, and tholeiitic magmatic rocks using this Streckeisen-style lithogeochemical classification procedure. In addition, classification of both felsic and mafic volcanic rocks have been achieved, also with positive results, suggesting that this lithogeochemical classification application may represent a new way and reliable way of classifying aphyric volcanic rocks. Finally, classification of ore-bearing and hydrothermally altered igneous rocks has been undertaken, and has provided not only accurate classifications, but also new insights into hydrothermal alteration processes.

References

CHAMPION, D.C., BUDD, A.R., HAZELL, M.S., SEDGMEN, A. 2007. OZCHEM: National Whole Rock Geochemistry Dataset. Geoscience Australia. http://www.ga.gov.au/ metadata-gateway/metadata/record/65464/.

COULSON, I.M., VILLENEUVE, M.E., DIPPLE, G.M., DUNCAN, R.A., RUSSELL, J.K., MORTENSEN, J.K. 2002. Time-scales of assembly and thermal history of a composite felsic pluton: Constraints from the Emerald Lake area, northern Canadian Cordillera, Yukon. *Journal of Volcanology and Geothermal Research*, **114**, 331-356.

COULSON, I.M., DIPPLE, G.M., RAUDSEPP, M. 2001. Evolution of HF and HCl activity in magmatic volatiles of the gold- mineralized Emerald Lake pluton, Yukon Territory, Canada. *Mineralium Deposita*, **36**, 594-606.

DUNCAN, R.A., 1999. *Physical and Chemical Zonation in the Emerald Lake Pluton, Yukon Territory*. M.Sc. thesis, University of British Columbia, Vancouver.

DUNCAN, R.A., RUSSELL, J.K., HASTINGS, N.L., ANDERSON, R.G. 1998a. *Geology, mineralogy, geochemistry, and physical properties of the mid-Cretaceous Emerald Lake pluton, southeastern Yukon*. Geological Survey of Canada, OF 3571.

DUNCAN, R.A., RUSSELL, J.K., HASTINGS, N.L., ANDERSON, R.G. 1998b. Relationship between chemical composition, physical properties and geology of the mineralised Emerald Lake Pluton, Yukon. In: *Current Research, Part A*. Geological Survey of Canada, Paper 1998-1A, 1-11.

EWART, A. 1982. The mineralogy and petrology of Tertiary-Recent orogenic volcanic rocks, with special reference to the andesitic-basaltic compositional range. 25-95, In: THORP, R.S. (ed) *Orogenic Andesites and Related Rocks*. John Wiley and Sons, New York.

FLOYD, P.A., WINCHESTER, J.A. 1975. Magma type and tectonic setting discrimination using immobile elements. *Earth and Planetary Science Letters*, **27**, 211-218.

FROST, B.R., FROST, C.D. 2008. A geochemical classification for feldspathic igneous rocks. *Journal of Petrology*, **49**, 1955-1969.

GLEN, R.A., DAWSON, M.W., COLQUHOUN, G.P. 2006. Eastern Lachlan orogen geoscience database (on DVD-ROM) Version 2, NSW Department of Primary Industries – Minerals, Geological Survey of New South Wales, Maitland, Australia.

HALLBERG, J.A. 1984. A geochemical aid to igneous rock identification in deeply weathered terrain. *Journal of Geochemical Exploration*, **20**, 1-8.

HOLLINGS, P., WYMAN, D. 2005. The geochemistry of trace elements in igneous systems: Principles and examples from basaltic systems. 1-24, In: LINNEN, R.,

SAMSON, I. (eds), *Rare Element Geochemistry and Ore Deposits*, Geological Association of Canada Short Course Notes, **17**.

IRVINE, T.N., BARAGAR, W.R.A. 1971. A guide to the chemical classification of the common volcanic rocks. *Canadian Journal of Earth Sciences*, **8**, 523-548.

LE BAS, M.J., LEMAITRE, R.W., STRECKEISEN, A., ZANETTIN, B. 1986. A chemical classification of volcanic rocks based on the total alkali-silica diagram. *Journal of Petrology*, **27**, 745-750.

LE MAITRE, R.W. 1976. The chemical variability of some common igneous rocks. *Journal of Petrology*, **17:4**, 589-637.

MCCALLUM, I.S., RAEDEKE, L.D., MATHEZ, E.A. 1980. Investigations of the Stillwater complex: Part I. Stratigraphy and structure of the banded zone. In: IRVING, A.J., DUNGAN, M.A. (eds), *American Journal of Science*, **280-A**, 59-87.

MCCORMACK, C., 1985. *Oberon Granites*. Unpublished B.Sc. thesis, Australian National University, Canberra. 42 p.

MESCHEDE, M. 1986. A method of discriminating between different types of mid-ocean ridge basalts and continental tholeiites with the Nb-Zr-Y diagram. *Chemical Geology*, **56**, 207-218.

MEURIER, W.P. 1995. *Postcumulus processes in layered intrusions: Theory and application of the Middle Banded series of the Stillwater complex, Montana*. Unpublished Ph.D. thesis, Duke University, Durham, North Carolina, 418 p.

MEURIER, W.P., BOUDREAU, A.E. 1998. Compaction of igneous cumulates, Part I: Geochemical consequences for cumulates and liquid fractionation trends. *Journal of Geology*, **106**, 281-292.

MEURIER, W.P., BOUDREAU, A.E. 1996. Petrology and mineral compositional features of the olivine-bearing zones of the Middle Banded series, Stillwater complex, Montana. *Journal of Petrology*, **37**, 583-607.

MIYASHIRO, A. 1974. Volcanic rock series in island arcs and active continental margins. *American Journal of Science*, **274**, 321-355.

PEARCE, J.A. 1996. A user's guide to basalt discrimination diagrams. 79-113, In: WYMAN, D.A. (ed). *Trace Element Geochemistry of Volcanic Rocks: Applications for Massive Sulphide Exploration*. Geological Association of Canada, Short Course Notes, **12**, Winnipeg, Manitoba.

PEARCE, J.A. 1983. Role of the sub-continental lithosphere in magma genesis at active continental margins. 230-249, In: HAWKSWORTH, C.J., NORRY, M.J. (eds), *Continental Basalts and Mantle Xenoliths*. Shiva Publishing Ltd., Cambridge, Mass.

PEARCE, J.A., ALABASTER, T., SCHETON, A.W., SEARLE, M.P. 1981. The Oman ophiolite as a Cretaceous arc-basin complex: Evidence and implications. *Philosophical Transactions*, Royal Society of London, 299-317.

PEARCE, J.A., CANN, J.R. 1973. Tectonic setting of basic volcanic rocks determined using trace element analyses. *Earth and Planetary Science Letters*, **19**, 290-300.

PEARCE, J.A., HARRIS, N.B.W., TINDLE, A.G. 1984. Trace element discrimination diagrams for the tectonic interpretation of granitic rocks. *Journal of Petrology*, **25**, 956-983.

POGSON, D. J., WATKINS, J, J. 1998. *Bathurst 1:250,000 Geological Sheet SI/55-8: Explanatory Notes*. Geological Survey of New South Wales, Sydney, 430 pp.

SHERVAIS, J.W. 1982. Ti-V plots and the petrogenesis of modern and ophiolitic lavas. *Earth and Planetary Science Letters*, **59**, 101-118.

SMIT, H. 1984. *Petrology, chemistry, age, and isotope study of the high potassium Emerald Lake pluton, eastern Yukon Territory*. B.Sc. thesis, University of British Columbia, Vancouver.

SMIT, H., ARMSTRONG, R.L., VAN DER HEYDEN, P. 1985. Petrology, chemistry and radiogenic isotope (K-Ar, Rb-Sr, and U-Pb) study of the Emerald Lake pluton, eastern Yukon Territory. In: *Current Research, Part B*. Geological Survey of Canada, Paper 85-1B, 347-359.

STANLEY, C.R. 2007. The fundamental relationship between sample mass and sampling variance in real geological samples and corresponding statistical models. *Geochemistry: Exploration, Environment, Analysis*, **16:1-2**, 109-123.

STRECKEISEN, A.L., ZANETTIN, B.A., LE BAS, M.J., BONIN, B., BATEMAN, P., BELLIENI, G., DUDE, A., EFREMOVA, S., KELLER, J., LAMEYRE, J., SABINE, P.A., SCHMID, R., SORENSEN, H., WOODLEY, A.R. 2002. *Igneous rocks; a classification and glossary of terms; recommendations of the International union of Geological Science Subcommission on the Systematics of Igneous Rocks*. Cambridge University Press, Cambridge, U.K., 800 p.

STRECKEISEN, A. 1974. Classification and nomenclature of plutonic rocks: Recommendations of the IUGS subcommission on the systematics of igneous rocks. *Geologische Rundschau*, **63**, 773-786.

SUN, S.S., MCDONOUGH, W.F. 1989. Chemical and isotopic systematics of oceanic basalts: Implications for mantle composition and processes. 313-345, In: SAUNDERS, A.D., NORRY, M.J. (eds), *Magmatism in the Ocean Basins*. Geological Society of London, **42**.

WINCHESTER, J.A., FLOYD, P.A. 1977. Geochemical discrimination of different magma series and their differentiation products using immobile elements. *Chemical Geology*, **20**, 325-343.

WOOD, D.A. 1980. The application of a Th-Hf-Ta diagram to problems of tectonomagmatic classification and to establishing the nature of crustal contamination of basaltic lavas on the British tertiary volcanic province. *Earth and Planetary Science Letters*, **50**, 11-30.

WYMAN, D.A., HOLLINGS, P. 2006. Late Archean convergent margin volcanism in the Superior province: A comparison of the Blake River group and Confederation assemblage. 215 – 238, In: Benn, K., Mareschal, J.C., Condie, K. (eds), *Archean Geodynamics and Environments*, American Geophysical Union, Monograph **164**.